

Reactor neutrino background in next-generation dark matter detectorsD. Aristizabal Sierra,^{1,*} V. De Romeri^{2,†} and C. A. Ternes^{3,‡}¹*Universidad Técnica Federico Santa María, Departamento de Física Casilla 110-V, Avenida España 1680, Valparaíso, Chile*²*Instituto de Física Corpuscular (CSIC-Universitat de València), Parc Científic UV C/ Catedrático José Beltrán, 2 E-46980 Paterna (València), Spain*³*Istituto Nazionale di Fisica Nucleare (INFN), Laboratori Nazionali del Gran Sasso, 67100 Assergi, L'Aquila (AQ), Italy*

(Received 14 February 2024; accepted 28 May 2024; published 24 June 2024)

Third-generation dark matter detectors will be fully sensitive to the ^8B solar neutrino flux. Because of this, the characterization of such a background has been the subject of extensive analyses over the last few years. In contrast, little is known about the impact of reactor neutrinos. In this paper, we report on the implications of such a flux for dark matter direct-detection searches. We consider five potential detector deployment sites envisioned by the recently established XLZD Consortium: SURF, SNOLAB, Kamioka, LNGS, and Boulby. By using public reactor data, we construct five reactor clusters—involving about 100 currently operating commercial nuclear reactors each—and determine the net neutrino flux at each detector site. Assuming a xenon-based detector and a 50 ton-year exposure, we show that in all cases the neutrino event rate may be sizable, depending on energy recoil thresholds. Of all possible detector sites, SURF and LNGS are those with the smallest reactor neutrino background. On the contrary, SNOLAB and Boulby are subject to the strongest reactor neutrino fluxes, with Kamioka being subject to a more moderate background. Our findings demonstrate that reactor neutrino fluxes should be taken into account in the next round of dark matter searches. We argue that this background may be particularly relevant for directional detectors, provided they meet the requirements we have employed in this analysis.

DOI: [10.1103/PhysRevD.109.115026](https://doi.org/10.1103/PhysRevD.109.115026)**I. INTRODUCTION**

A wealth of cosmological and astrophysical observations [1] supports the idea that the dominant form of matter in the Universe is of unknown origin, with feeble or no electromagnetic interactions. Models in which this dark matter (DM) is mainly nonbaryonic and instead made up of new subatomic particles seem to better comply with all experimental hints. On the other hand, little is known about the underlying Standard Model (SM) extension that can accommodate DM, barring a few requirements that such a new particle should fulfill to be a viable DM candidate.

One compelling solution are weakly interacting massive particles (WIMPs). Their annihilation cross section is similar in strength to electroweak interactions, and it is

sufficiently large to allow it to reach thermal equilibrium with the SM plasma in the early Universe. In such a scenario, an accurate prediction of the measurable relic density can be obtained, turning out to be compatible with astrophysical and cosmological observations in a standard cosmological model (for a review, see, e.g., Refs. [2,3]). Besides the theoretical motivations, WIMPs are appealing also because of their testability.

Should they interact with SM particles, one strategy that has been envisaged for their search is direct detection (DD). This technique is based on the assumption that DM particles in the Galactic halo may scatter with the target material inside underground, voluminous detectors while crossing the Earth [4,5]. This idea was first put forward by Goodman and Witten in the mid-1980s, pointing out that WIMPs could be searched for by using the same detectors proposed by Drukier and Stodolsky for coherent elastic neutrino-nucleus scattering (CE ν NS) measurements [6,7]. In the case of WIMPs, they would undergo scattering on the nuclei and electrons of the target material, the signature being a recoil of tiny energy. Despite the huge experimental effort devoted to these searches in the past years, no positive signal has been found to date [8]. Conversely and as a byproduct, detector technologies as

*daristizabal@uliege.be

†deromeri@ific.uv.es

‡christoph.ternes@lngs.infn.it

Published by the American Physical Society under the terms of the [Creative Commons Attribution 4.0 International license](https://creativecommons.org/licenses/by/4.0/). Further distribution of this work must maintain attribution to the author(s) and the published article's title, journal citation, and DOI. Funded by SCOAP³.

well as fiducial volumes of DD experiments have dramatically evolved.

At present, DM searches in DD experiments are led by liquid xenon (LXe) dual-phase time projection chambers (second-generation DM detectors). Detectors at the INFN “Laboratori Nazionali del Gran Sasso” (LNGS) in Italy (XENONnT), at the Sanford Underground Research Facility (SURF) in South Dakota in the U.S. (LZ), and at the China Jinping Underground Laboratory in Sichuan, China (PandaX-4T), are using active volumes of the order of 5 tons [9–11]. The high capabilities for background rejection, and the low nuclear recoil energy thresholds, allow these second-generation DM detectors to be sensitive to spin-independent WIMP-nucleon total cross sections of the order of 10^{-48} cm² [8]. Indeed, XENONnT and LZ have recently published results where sensitivities of the order of $\sigma_{\text{WIMP-nuc}} \sim 10^{-47}$ cm² have been reported [9,10]. PandaX-4T has set the most stringent upper limit in the low WIMP mass region ($\lesssim 10$ GeV), $\sigma_{\text{WIMP-nuc}} \sim 10^{-44}$ cm² [11].

A new generation of LXe detectors—third-generation DM detectors—is expected to pave the way for a discovery. Note that if a discovery should take place in second-generation detectors, the experimental environment provided by their third-generation follow-ups will allow precise measurements of WIMP properties. Recently, the XENONnT, LZ, and DARWIN Collaborations have united forces and created the XLZD Consortium [12]. Their goal is the construction of a 40–100 ton detector with unprecedented sensitivities. With such active volume, a detector of this kind will be subject to an irreducible neutrino background dominated by ⁸B solar neutrinos (for nuclear-channel signals) and by pp neutrinos (for electron-channel signals) [13]. The Sun is not the only source of background neutrinos, though. Other astrophysical sources, like the diffuse supernova neutrino background and atmospheric neutrinos, are expected to affect and complicate WIMP searches at DD experiments. However—as is well known—in third-generation LXe detectors, the background will be dominated by ⁸B neutrinos: with recoil-energy thresholds of $\sim \mathcal{O}(1)$ keV, only fluxes with energies above a few MeV can generate measurable recoils. In that energy range, the ⁸B flux dominates by about 3 orders of magnitude over the *hep* flux. Sizable signals generated by fluxes other than the ⁸B component will require much larger exposures.

The morphology and size of these backgrounds have been the subject of different analyses in recent years, first identified as the so-called “neutrino floor” [13–17] and its more recent redefinition, the “neutrino fog” [18], where a first estimation of the reactor neutrino background at LNGS was addressed. For a description of the neutrino floor as described by effective nuclear calculations, we refer the interested reader to Ref. [19]. It is well known that the impact of the neutrino background on a WIMP discovery

signal is mainly dominated by neutrino flux uncertainties, as the uncertainties on the weak mixing angle and on the root-mean-square radii of the neutron distributions play a rather subdominant role [20]. The uncertainty on the ⁸B neutrino flux is obtained by a combined analysis of solar neutrino data from all phases of the Sudbury Neutrino Observatory and amounts to about 4% [21]. This result improves previous uncertainties derived from single-phase analyses while being consistent with solar model predictions [22]. The presence of a neutrino background, however, does not mean that the identification of a WIMP signal is impossible. First of all, improvements in the determination of solar neutrino flux uncertainties are expected. Second, WIMP and neutrino spectra in general do not fully degenerate in most regions of parameter space. Even in regions where they strongly do, an identification is possible with sufficiently large datasets [16]. Furthermore, even if data are not abundant, directionality will—potentially—enable a distinction between WIMP and neutrino nuclear recoil spectra [23], if they turn out to be strongly degenerate.

Given this landscape, and the fact that DM direct detection will soon enter the third-generation detector phase, one should wonder whether other neutrino sources—including artificial ones—might contribute to the background and hence should be taken into account. This is a rather relevant question to raise, aiming to leverage the full discovery power of these types of detectors. Motivated by this question, in this paper we assess the impact of nuclear reactor antineutrinos. Neutron-rich unstable nuclei produced in fission processes of ²³⁵U, ²³⁸U, ²³⁹Pb, and ²⁴¹Pb generate via β decay a large electron antineutrino flux (see, e.g., [24]). Since more than ten years ago, theoretical calculations of the $\bar{\nu}_e$ flux have been shown to disagree with its measurement at the $\sim 5\%$ level [25]. Recently, however, in the light of new $\bar{\nu}_e$ flux calculations, the statistical significance of this discrepancy has been proven to be dramatically reduced [26,27]. The reactor neutrino flux is not universal but strongly depends on the geographical position of the detector. For definitiveness, we use LNGS (Italy), SURF (USA), Boulby (United Kingdom), Kamioka (Japan), and SNOLAB (Canada) as possible deployment sites. These underground facilities are considered as potential locations for detector deployment by the XLZD Consortium [12].

Our paper is structured as follows: In Sec. II, we present our analysis strategy; in Sec. III, we discuss our results; and we conclude in Sec. IV.

II. ANALYSIS STRATEGY

In this section, we explain the analysis strategy and how to calculate the number of reactor neutrino events in xenon detectors.

The datasets that we employ follow from data provided on the Geoneutrinos.org website [28,29]. This website

TABLE I. Minimum and maximum baselines (L_{\min} and L_{\max}) along with minimum and maximum reactor powers (P_{\min} and P_{\max}) for the SURF, SNOLAB, Kamioka, LNGS, and Boulby reactor clusters. The number of reactors in each cluster (NR) is also shown. Data have been extracted from the Geoneutrinos.org website.

Location	NR	L_{\min} [km]	L_{\max} [km]	P_{\min} [GW]	P_{\max} [GW]
SURF	111	790	2951	0.34	3.9
SNOLAB	104	239	2874	0.92	3.9
Kamioka	86	146	2895	0.15	3.9
LNGS	146	417	4027	0.42	3.7
Boulby	141	26	3654	0.51	3.7

contains valuable information on the global nuclear reactor network. We have extracted the thermal power and geographical position (and hence the distance to each detector site) for each reactor from this website. We consider only commercial power plants (that involve the most powerful reactors) for which a nonzero operating power is reported. Reactors for which the thermal capacity is known, but that have zero operating power, and those that have been permanently shut down are not included. Depending on the baseline, each detector site that we consider is “surrounded” by a cluster of nuclear reactor power plants, at a certain distance L_i . Table I shows the minimum and maximum baseline and power for each cluster, along with the number of reactors involved. For each detector site, we do not include reactors located at distances beyond L_{\max} , as their contribution to the event rates would be negligible.

The largest clusters are those around the LNGS and Boulby detector sites (as expected, given that for these two

cases the radius defining the cluster exceeds by about 1000 km the radius at the other sites). However, this does not necessarily mean that the largest flux is obtained for these two positions, as we now discuss. The reactor neutrino flux decreases rapidly with increasing baseline. So, a rather fair assumption is that the flux is dominated by the subcluster defined by all reactors included in a radius $\lesssim 1000$ km. For the SURF and LNGS locations, one finds that these subclusters involve only five reactors with a 2.1 and 1.8 GW average power, respectively. For the Kamioka, SNOLAB, and Boulby locations, the subclusters are composed, instead, of 35, 59, and 49 reactors. The average power in each case (and in that order) is 2.1 GW, 2.7 GW, and 1.9 GW. Thus, already from these numbers, one expects the SURF and LNGS location sites to involve a less intense reactor neutrino flux.

Figure 1 shows the distribution of nuclear reactors in terms of baseline and power for the five different clusters we consider. The distributions involve the full datasets. From the graph, one can see that for the Boulby and SNOLAB clusters, the reactor density for baselines below 1000 km is high, with a few of those reactors having powers above 3 GW. The distribution for the Kamioka cluster is somewhat different. Although below 1000 km there are a few reactors, their density is lower, as well as their power. For the SURF and LNGS clusters, the reactor density for baselines below 1000 km is, instead, rather moderate. For these clusters, most reactors are at baselines above 1000 km. So, even without a dedicated calculation of the event rate, expectations are that in terms of increasing reactor neutrino fluxes, the clusters can be sorted into three groups: SURF/LNGS, Kamioka, and SNOLAB/Boulby.

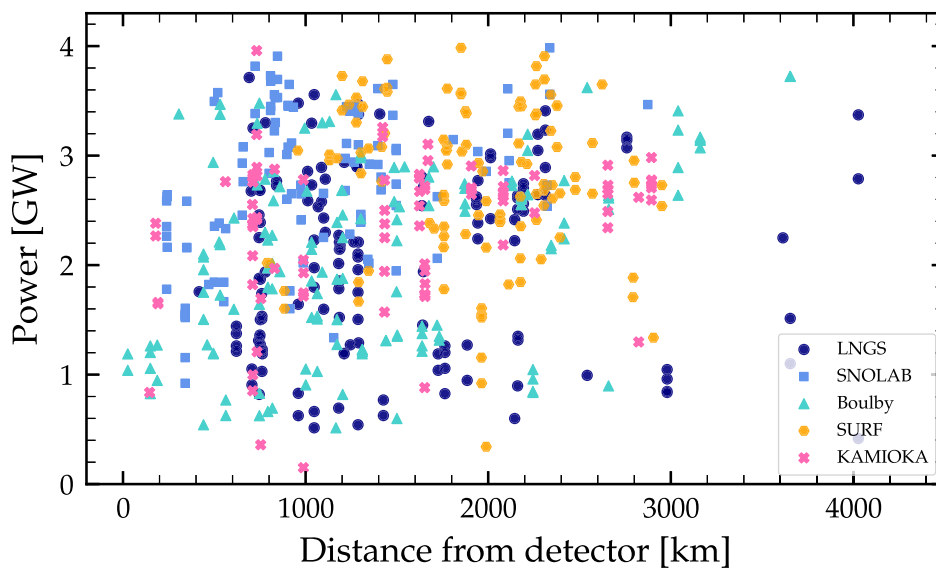


FIG. 1. Operating power and distance of different reactors (organized in clusters, see Table I) that may affect five possible deployment sites of third-generation detectors—i.e., SURF (USA), SNOLAB (Canada), Kamioka (Japan), LNGS (Italy), and Boulby (United Kingdom).

The calculation of the differential nuclear recoil spectrum at each cluster (C) requires the convolution of the differential CE ν NS cross section [7,30] with the reactor neutrino flux, namely

$$\frac{dR_C}{dE_r} = \frac{m_{\text{det}} N_A T \eta_C}{m_{\text{mol}}^{\text{Xe}}} \int_{E_\nu^{\text{min}}}^{E_\nu^{\text{max}}} \frac{d\Phi_{\bar{\nu}_e}}{dE_\nu} \frac{d\sigma}{dE_r} F_H^2(E_r) dE_\nu. \quad (1)$$

Here, m_{det} refers to the detector active volume mass, $m_{\text{mol}}^{\text{Xe}}$ to the xenon molar mass, T to the exposure time, $E_\nu^{\text{min}} = \sqrt{m_N E_r / 2}$ (E_r and m_N refer to nuclear recoil energy and mass), and E_ν^{max} refers to the neutrino spectrum kinematic “high-energy” tail taken at 8 MeV. The average nuclear mass is $\langle m_{\text{Xe}} \rangle / \text{GeV} = 0.93 \times \langle A \rangle$, with $\langle A \rangle = \sum_i X_i A_i = 131.4$ being the mass number averaged over the nine stable xenon isotopes. We include—for completeness—the weak-charge nuclear form factor, $F_H(E_r)$, parametrized *à la* Helm [31]. Note that if it were not included, results would deviate from those presented here at most by $\sim 2\%$, because of the process occurring deep in the full coherent regime.

Regarding the electron antineutrino spectrum, we proceed as follows. For the ^{235}U and ^{238}U emission spectra, we use results from Ref. [32]. For ^{239}Pu and ^{241}Pu , we use instead results from Ref. [33]. The reactor neutrino flux is obtained from the decays of the daughters of the fission products of these four isotopes (see Ref. [34] for a recent review). In Refs. [32,33] (see also Refs. [35,36]), the neutrino fluxes are obtained by converting the measured beta spectra into neutrino spectra. This method used to obtain the neutrino fluxes is called the “conversion method.” It is also possible to calculate the neutrino fluxes directly using information (decay chains, branching ratios, etc.) from the nuclear database and summing all branches together. This so-called “summation method” was used to obtain the fluxes obtained in Refs. [37,38]. As of today, both the conversion method and summation method produce similar results regarding the neutrino fluxes [27]. The full electron antineutrino differential flux is calculated according to

$$\frac{d\Phi_{\bar{\nu}_e}}{dE_\nu} = \sum_{i=\text{Isotopes}} f_i \frac{d\Phi_{\bar{\nu}_e}^i}{dE_\nu}, \quad (2)$$

where $f_i = \{f^{235\text{U}}, f^{238\text{U}}, f^{239\text{Pu}}, f^{241\text{Pu}}\} = \{5.5, 0.7, 3.2, 0.6\} \times 10^{-1}$ are the uranium and plutonium fission fractions [39]. We assume the spectral function in Eq. (2) to be universal for all the reactors within the clusters. In fact, each reactor has its own fission fractions, but variations are at the per-mille level (see, e.g., Table 4 in Ref. [27]). Thus, the difference among clusters is determined only by the normalization factor, which we calculate assuming that in each fission process an energy of $\epsilon = 205.24$ MeV is released, and that neutrinos are emitted isotropically. Explicitly, each normalization factor is given by

TABLE II. Neutrino flux normalization factors for the five reactor clusters.

Cluster	SURF	SNOLAB	Kamioka	LNGS	Boulby
$\eta_C [\text{cm}^{-2} \text{sec}^{-1}]$	20422	156630	103903	56677	932874

$$\eta_C = \sum_j \frac{P_j}{4\pi L_j^2 \epsilon}, \quad (3)$$

where j runs over all reactors relevant for cluster C, and P_j and L_j are the operating power and distance for reactor j . Their values are displayed in Table II, showing that SURF is subject to the least abundant neutrino flux, whereas Boulby is subject to the most severe.

With these results at hand, we are now in a position to calculate the differential event rate, as well as the total event rate, for each detector site. We assume a 50-ton active-volume LXe detector and 100% efficiency. Note that the XLZD Consortium aims at masses from 40 to 100 tons. So this value is used just as a proxy of what the actual detector will use. Since current realistic thresholds amount to 0.3 keV [40], we use $E_r^{\text{th, min}} = 0.1$ keV as a value envisioned for future detector operations. Results are displayed in Fig. 2. The left (right) graph shows the differential event rate (total event rate) as a function of the recoil energy (recoil energy threshold) for the five different reactor clusters we have considered. The inset plot in the right panel is meant to zoom in on the bottom-left corner. In line with expectations, the differential and total event rates at the SURF (Boulby) detector site are the smallest (largest). The event rate at the LNGS detector location is slightly higher, followed by Kamioka and SNOLAB.

III. DISCUSSION

Naively, one would expect the reactor neutrino flux to be suppressed and of little relevance. This expectation is mainly based on the fact that most reactors are far away from the detector sites. However, the fact that the clusters around each detector site involve a large number of active nuclear power plants (with, in some cases, powerful reactors), combined with a large active volume, produces a nonzero event rate in all cases.

Ideally, one would like a very low threshold to explore the small WIMP mass window and increase the WIMP-nucleus event rate. At 0.1 keV, we find that the total neutrino-nucleus event rate per year is 16 (SURF), 44 (LNGS), 82 (Kamioka), 124 (SNOLAB), and 733 (Boulby). If that operation threshold is not achieved and instead the detector is operated at 0.3 keV, these numbers will be degraded by about a factor of 7. In such an experimental scenario, the reactor neutrino background becomes, of course, less severe. Thus, the question of

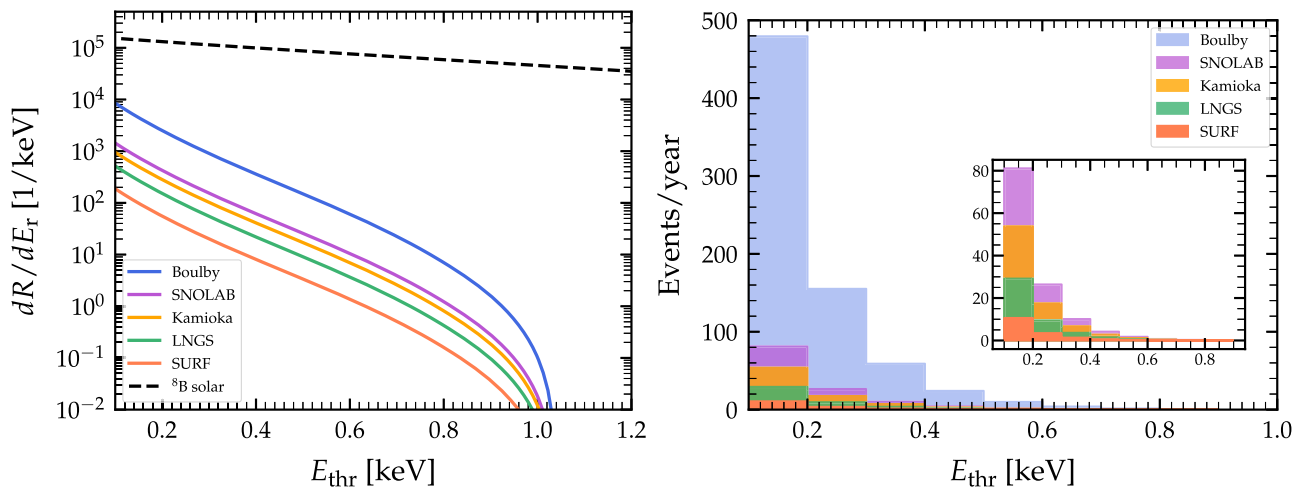


FIG. 2. Left graph: reactor neutrino differential event rate for the five detector sites considered in this work: SURF, SNOLAB, Kamioka, LNGS, and Boulby as a function of nuclear recoil energy. Shown as well is the ^8B differential event rate. Right graph: reactor neutrino total event rate for the same detector locations. The inset plot is a zoom-in on the bottom-left corner.

whether the reactor neutrino background matters is—as anticipated—strongly linked to operation thresholds.

It is worth emphasizing that variations of these estimated numbers are expected in the future, depending on the exact number of reactors that enter in either operation phase or are decommissioned. However, these results demonstrate that the reactor neutrino flux should be seriously taken into account in decision-making, as well as in data taken, contrary to expectations.

Finally, one might wonder how much this neutrino background matters compared to the ^8B solar neutrino flux (measured in several experiments [41–45]). For the detector configurations we have considered, with a 0.1 keV operation threshold, the number of ^8B nuclear recoil induced events is overwhelming, 36500 events/year. A precise calculation of this number requires folding the ^8B neutrino flux with the $\text{CE}\nu\text{NS}$ cross section and integrating over the recoil energy with a threshold of 0.1 keV. An order-of-magnitude estimation is, however, possible by rescaling results from Ref. [16] by the corresponding exposure. So, of course, this will be the dominant background source. All the efforts to understand the morphology of this background are indeed motivated by this fact. The question is then whether one should be concerned with the reactor neutrino background whatsoever.

It is well known that the ^8B background can be to a certain degree circumvented. As we have already stressed, large datasets might enable differentiating neutrinos from WIMP signals, if the WIMP parameters are such that the neutrino and WIMP event rates strongly degenerate. In general, however, directional detectors seem to be the most promising avenue [23,46]. They have been, as well, recently considered for $\text{CE}\nu\text{NS}$ measurements and beyond the SM searches using neutrino beamlines at Fermilab [47–49]. For these detectors, it seems that the

reactor neutrino background might even become the most dominant background source. Therefore, if the ^8B nuclear recoil-induced events can be efficiently discriminated, there will be yet another background source that will require careful identification and proper treatment, depending on statistics and operation capabilities.

IV. CONCLUSIONS

With the advent of third-generation DM direct-detection detectors, the quantification of reactor neutrino fluxes becomes of pivotal importance. In this work, we have quantified the size of the neutrino flux produced by clusters of reactors surrounding five potential detector deployment sites. For definitiveness, we have considered the locations envisioned by the recently established XLZD Consortium: SURF, SNOLAB, Kamioka, LNGS, and Boulby.

Our findings show that detectors with active volumes of the order of 50 tons and recoil energy thresholds of the order of 0.1 keV will be sensitive to a certain amount of reactor neutrino-induced events. The exact amount depends, to a large degree, on the energy threshold at which the detector is operated. However, even assuming a realistic threshold of 0.3 keV, the event rate turns out to be sizable in all cases. We find that the site with the smallest reactor neutrino background is SURF, followed by LNGS, Kamioka, SNOLAB, and Boulby (in that order).

Although subdominant compared to the solar ^8B neutrino background, we point out that the reactor neutrino background (and its corresponding events) should be—in principle—considered during data taken. Reactor neutrino-induced events should be taken into account in background discrimination, regardless of the detector technique employed. This result will be particularly relevant for

directional detection, if future detectors meet the requirements we have used here.

ACKNOWLEDGMENTS

We thank P. Martínez-Miravé for pointing out the Geoneutrinos.org website. The work of D. A. S. is funded by ANID under Grant “Fondecyt Regular” No. 1221445. He thanks “Le Service de Physique Théorique (Université Libre de Bruxelles)” and “Instituto de Física Corpuscular

(CSIC y Universidad de Valencia)” for their kind hospitality and their stimulating research environment during the completion of this work. V. D. R. acknowledges financial support from the CIDEXG/2022/20 grant (project “D’AMAGAT”) funded by Generalitat Valenciana and by Spanish Grant No. PID2020–113775 GB-I00 (MCIN/AEI/10.13039/501100011033). C. A. T. is very thankful for the hospitality at Universidad Técnica Federico Santa María, where this work was initiated.

-
- [1] N. Aghanim *et al.* (Planck Collaboration), Planck 2018 results: VI. Cosmological parameters, *Astron. Astrophys.* **641**, A6 (2020); **652**, C4(E) (2021).
- [2] G. Arcadi, M. Dutra, P. Ghosh, M. Lindner, Y. Mambrini, M. Pierre, S. Profumo, and F. S. Queiroz, The waning of the WIMP? A review of models, searches, and constraints, *Eur. Phys. J. C* **78**, 203 (2018).
- [3] G. Arcadi, D. Cabo-Almeida, M. Dutra, P. Ghosh, M. Lindner, Y. Mambrini, J. P. Neto, M. Pierre, S. Profumo, and F. S. Queiroz, The waning of the WIMP: Endgame?, [arXiv:2403.15860](https://arxiv.org/abs/2403.15860).
- [4] M. Schumann, Direct detection of WIMP dark matter: Concepts and status, *J. Phys. G* **46**, 103003 (2019).
- [5] D. Baxter *et al.*, Recommended conventions for reporting results from direct dark matter searches, *Eur. Phys. J. C* **81**, 907 (2021).
- [6] M. W. Goodman and E. Witten, Detectability of certain dark matter candidates, *Phys. Rev. D* **31**, 3059 (1985).
- [7] A. Drukier and L. Stodolsky, Principles and applications of a neutral current detector for neutrino physics and astronomy, *Phys. Rev. D* **30**, 2295 (1984).
- [8] J. Billard *et al.*, Direct detection of dark matter—APPEC Committee report*, *Rep. Prog. Phys.* **85**, 056201 (2022).
- [9] E. Aprile *et al.* (XENON Collaboration), First dark matter search with nuclear recoils from the XENONnT experiment, *Phys. Rev. Lett.* **131**, 041003 (2023).
- [10] J. Aalbers *et al.* (LZ Collaboration), First dark matter search results from the LUX-ZEPLIN (LZ) experiment, *Phys. Rev. Lett.* **131**, 041002 (2023).
- [11] S. Li *et al.* (PandaX Collaboration), Search for light dark matter with ionization signals in the PandaX-4T experiment, *Phys. Rev. Lett.* **130**, 261001 (2023).
- [12] The XLZD Consortium, <https://xlzd.org/>.
- [13] L. E. Strigari, Neutrino coherent scattering rates at direct dark matter detectors, *New J. Phys.* **11**, 105011 (2009).
- [14] J. Monroe and P. Fisher, Neutrino backgrounds to dark matter searches, *Phys. Rev. D* **76**, 033007 (2007).
- [15] J. D. Vergados and H. Ejiri, Can solar neutrinos be a serious background in direct dark matter searches?, *Nucl. Phys.* **B804**, 144 (2008).
- [16] J. Billard, L. Strigari, and E. Figueroa-Feliciano, Implication of neutrino backgrounds on the reach of next generation dark matter direct detection experiments, *Phys. Rev. D* **89**, 023524 (2014).
- [17] C. A. J. O’Hare, Dark matter astrophysical uncertainties and the neutrino floor, *Phys. Rev. D* **94**, 063527 (2016).
- [18] C. A. J. O’Hare, New definition of the neutrino floor for direct dark matter searches, *Phys. Rev. Lett.* **127**, 251802 (2021).
- [19] R. Essig, M. Sholapurkar, and T.-T. Yu, Solar neutrinos as a signal and background in direct-detection experiments searching for sub-GeV dark matter with electron recoils, *Phys. Rev. D* **97**, 095029 (2018).
- [20] D. Aristizabal Sierra, V. De Romeri, L. J. Flores, and D. K. Papoulias, Impact of COHERENT measurements, cross section uncertainties and new interactions on the neutrino floor, *J. Cosmol. Astropart. Phys.* **01** (2022) 055.
- [21] B. Aharmim *et al.* (SNO Collaboration), Combined analysis of all three phases of solar neutrino data from the Sudbury Neutrino Observatory, *Phys. Rev. C* **88**, 025501 (2013).
- [22] A. Serenelli, S. Basu, J. W. Ferguson, and M. Asplund, New solar composition: The problem with solar models revisited, *Astrophys. J. Lett.* **705**, L123 (2009).
- [23] S. E. Vahsen, C. A. J. O’Hare, and D. Loomba, Directional recoil detection, *Annu. Rev. Nucl. Part. Sci.* **71**, 189 (2021).
- [24] C. Bemporad, G. Gratta, and P. Vogel, Reactor based neutrino oscillation experiments, *Rev. Mod. Phys.* **74**, 297 (2002).
- [25] G. Mention, M. Fechner, T. Lasserre, T. A. Mueller, D. Lhuillier, M. Cribier, and A. Letourneau, The reactor antineutrino anomaly, *Phys. Rev. D* **83**, 073006 (2011).
- [26] J. M. Berryman and P. Huber, Reevaluating reactor antineutrino anomalies with updated flux predictions, *Phys. Rev. D* **101**, 015008 (2020).
- [27] C. Giunti, Y. F. Li, C. A. Ternes, and Z. Xin, Reactor antineutrino anomaly in light of recent flux model refinements, *Phys. Lett. B* **829**, 137054 (2022).
- [28] S. Dye and A. Barna, Global antineutrino modeling for a web application, [arXiv:1510.05633](https://arxiv.org/abs/1510.05633).
- [29] Geoneutrinos website, <https://reactors.geoneutrinos.org/>.
- [30] D. Z. Freedman, Coherent neutrino nucleus scattering as a probe of the weak neutral current, *Phys. Rev. D* **9**, 1389 (1974).

- [31] R. H. Helm, Inelastic and elastic scattering of 187-MeV electrons from selected even-even nuclei, *Phys. Rev.* **104**, 1466 (1956).
- [32] V. Kopeikin, M. Skorokhvatov, and O. Titov, Reevaluating reactor antineutrino spectra with new measurements of the ratio between ^{235}U and ^{239}Pu β spectra, *Phys. Rev. D* **104**, L071301 (2021).
- [33] P. Huber, On the determination of anti-neutrino spectra from nuclear reactors, *Phys. Rev. C* **84**, 024617 (2011); **85**, 029901(E) (2012).
- [34] A. C. Hayes and P. Vogel, Reactor neutrino spectra, *Annu. Rev. Nucl. Part. Sci.* **66**, 219 (2016).
- [35] T. A. Mueller *et al.*, Improved predictions of reactor anti-neutrino spectra, *Phys. Rev. C* **83**, 054615 (2011).
- [36] L. Hayen, J. Kostensalo, N. Severijns, and J. Suhonen, First-forbidden transitions in the reactor anomaly, *Phys. Rev. C* **100**, 054323 (2019).
- [37] M. Estienne *et al.*, Updated summation model: An improved agreement with the Daya Bay antineutrino fluxes, *Phys. Rev. Lett.* **123**, 022502 (2019).
- [38] L. Perissé, A. Onillon, X. Mougeot, M. Vivier, T. Lasserre, A. Letourneau, D. Lhuillier, and G. Mention, Comprehensive revision of the summation method for the prediction of reactor $\bar{\nu}_e$ fluxes and spectra, *Phys. Rev. C* **108**, 055501 (2023).
- [39] H. T. Wong *et al.* (TEXONO Collaboration), A search of neutrino magnetic moments with a high-purity germanium detector at the Kuo-Sheng Nuclear Power Station, *Phys. Rev. D* **75**, 012001 (2007).
- [40] B. Lenardo *et al.*, Measurement of the ionization yield from nuclear recoils in liquid xenon between 0.3–6 keV with single-ionization-electron sensitivity, [arXiv:1908.00518](https://arxiv.org/abs/1908.00518).
- [41] S. Fukuda *et al.* (Super-Kamiokande Collaboration), Solar ^8B and hep neutrino measurements from 1258 days of Super-Kamiokande data, *Phys. Rev. Lett.* **86**, 5651 (2001).
- [42] S. Abe *et al.* (KamLAND Collaboration), Measurement of the ^8B solar neutrino flux with the KamLAND liquid scintillator detector, *Phys. Rev. C* **84**, 035804 (2011).
- [43] M. Agostini *et al.* (Borexino Collaboration), Improved measurement of ^8B solar neutrinos with 1.5kt \cdot y of Borexino exposure, *Phys. Rev. D* **101**, 062001 (2020).
- [44] B. Aharmim *et al.* (SNO Collaboration), Measurement of the ν_e and total ^8B solar neutrino fluxes with the Sudbury Neutrino Observatory phase-III data set, *Phys. Rev. C* **87**, 015502 (2013).
- [45] M. Anderson *et al.* (SNO+ Collaboration), Measurement of the ^8B solar neutrino flux in SNO+ with very low backgrounds, *Phys. Rev. D* **99**, 012012 (2019).
- [46] S. E. Vahsen *et al.*, CYGNUS: Feasibility of a nuclear recoil observatory with directional sensitivity to dark matter and neutrinos, [arXiv:2008.12587](https://arxiv.org/abs/2008.12587).
- [47] M. Abdullah, D. Aristizabal Sierra, B. Dutta, and L. E. Strigari, Coherent elastic neutrino-nucleus scattering with directional detectors, *Phys. Rev. D* **102**, 015009 (2020).
- [48] D. Aristizabal Sierra, B. Dutta, D. Kim, D. Snowden-Ifft, and L. E. Strigari, Coherent elastic neutrino-nucleus scattering with the $\nu\text{BDX-DRIFT}$ directional detector at next generation neutrino facilities, *Phys. Rev. D* **104**, 033004 (2021).
- [49] D. Aristizabal Sierra, J. L. Barrow, B. Dutta, D. Kim, D. Snowden-Ifft, L. Strigari, and M. H. Wood ($\nu\text{BDX-DRIFT}$ Collaboration), Rock neutron backgrounds from FNAL neutrino beamlines in the $\nu\text{BDX-DRIFT}$ detector, *Phys. Rev. D* **107**, 013003 (2023).